Low Temperature Physics/Fizika Nizkikh Temperatur, 2015, v. 41, No. 10, pp. 984–988

Magnetic states in multiply-connected flat nanoelements

Andrei B. Bogatyrev

Institute for Numerical Mathematics, Russian Academy of Sciences, 8 Gubkina Str., Moscow 119991, Russia

Konstantin L. Metlov

Donetsk Institute for Physics and Engineering of the National Academy of Sciences of Ukraine
46 Nauki Ave., Kyiv 03680, Ukraine
E-mail: metlov@fti.dn.ua

Received April 5, 2015, published online August 25, 2015

Flat magnetic nanoelements are an essential component of current and future spintronic devices. By shaping an element it is possible to select and stabilize chosen metastable magnetic states, control its magnetization dynamics. Here, using a recent significant development in mathematics of conformal mapping, complex variable based approach to the description of magnetic states in planar nanoelements is extended to the case when elements are multiply-connected (that is, contain holes or magnetic antidots). We show that presence of holes implies a certain restriction on the set of magnetic states of nanoelement.

PACS: 75.60.Ch Domain walls and domain structure;
75.70.Kw Domain structure (including magnetic bubbles and vortices);
85.70.Kh Magnetic thin film devices: magnetic heads (magnetoresistive, inductive, etc.); domain-motion devices, etc.

Keywords: micromagnetics, nanomagnetics, magnetic nanodots.

While existence of topological solitons [1] as metastable states in infinite 2nd ferromagnets was known theoretically for quite a long time [2–4], real systems have finite size. Their boundary imposes restrictions on the set of low-energy topological states, making it equivalent to the set of rational functions of complex variable with real coefficients [5], as opposed to complex coefficients in the laterally unconstrained thin film case [2]. Also, restricted geometry implies the possibility of formation of half-vortex states, pinned at the side of the planar magnet [6,5], which are topologically similar to the boundary states in the fractional quantum Hall systems and topological insulators. The shape of nanoelement enters this complex description [5] via its conformal mapping to the unit disk. It is also possible to express Landau–Lifshitz magnetization dynamics directly in terms of these complex functions using Lagrangian approach [7]. The complex description of magnetization states [5] and their dynamics [7,8] constitutes a complete set of analytical tools to study magnetic textures in simply-connected nanomagnets far from magnetic saturation. Here this description is extended for the case when planar nanomagnet is multiply-connected.

Let us briefly introduce the description for simply-connected case [5]. In small enough magnets the surface effects dominate the volume ones, and also the exchange interaction is more important than the magnetostatic one. The former is typical for any small systems, while the latter is easy to understand based on the representation of the magnetostatic energy in terms of the interaction of fictitious magnetic charges of opposite signs. The total magnetic charge is always zero, thus, whatever the distribution of the magnetization is, as the size of the magnet decreases, the positive and negative charges are brought closer together, so that their positive self-energy gets more and more compensated by their negative mutual interaction energy. The scaling of the exchange energy of the set of such an arbitrary magnetization distributions follows the volume of the magnet and does not have such an additional reduction. Thus, in small magnets the exchange interaction becomes more important. To make use of this energy hierarchy, we build an approximate expressions for magnetic states by minimizing the energy terms sequentially (as opposed to minimization of their sum, which would result in the exact theory). The process of sequential minimization is analogous to sieving.

First, consider all possible magnetization distributions with fixed length of magnetization vector $|\mathbf{m}|=1$:

$$m_X + im_Y = \frac{2w(z,\overline{z})}{1+w(z,\overline{z})\overline{w}(z,zc)}$$
$$m_Z = \frac{1-w(z,\overline{z})\overline{w}(z,zc)}{1-w(z,\overline{z})\overline{w}(z,zc)}, \quad (1)$$

where $\mathbf{m}=\{m_X, m_Y, m_Z\}=\mathbf{M}/M_S$ is the local magnetization vector, expressed in units of saturation magnetization M_S; $z=X+iY$, with X, Y and Z being the Cartesian coordinates (the element is assumed to be the a flat cylinder with axis, parallel to Z and magnetization distributions are assumed to be Z-independent), $w(z,\overline{z})$ is a function (not necessarily meromorphic) of complex variable z.

Second, out of all these functions select the ones, which, additionally to having the constant length of the magnetization, minimize the exchange energy (these are the famous Belavin and Polyakov solitons [2]). Then further restrict the set of the remaining functions twice by selecting those, which give minimum for the energies of face magnetic charges and those, which minimize (in fact, totally avoid) the side magnetic charges. The final result [5] of such a selection will be the following representation for $w(z,\overline{z})$

$$w(z,\overline{z})=\begin{cases} f(z)/e_1 & |f(z)|\le e_1 \\ f(z)/\sqrt{f(z)\overline{f}(\overline{z})} & e_1<|f(z)|\le e_2, \\ f(z)/e_2 & |f(z)|>e_2 \end{cases} \quad (2)$$

where e_1 and e_2 are real positive constants. The complex function $f(z)$ is a solution of Riemann–Hilbert boundary value problem of finding the meromorphic function in the domain D, which corresponds to the face of the planar nanoelement, having no normal components to the domain's boundary. This problem usually has many solutions. For simply-connected case their set is equivalent to the set of rational functions with real coefficients (constants), whose zeros(poles) correspond to vortex (antivortex) centers [5].

For example, in a unit disk the subset of states with no antivortices can be expressed [6] as

$$f^{\text{disk}}(z) = izc + A - \overline{A}z^2, \quad (3)$$

where c and A are a real and a complex constants respectively. While the equilibrium values of these constants can be found only by minimizing the total (including the energy of the volume magnetic charges) energy of the nanomagnet [9], the Ex. (3) can already be useful to pinpoint that there are several types of magnetic states in the disk, such as centered magnetic vortex (when $A=0$), the so-called "leaf" state (when $c=0$) and C-like magnetization state (when $4A\overline{A}>c$). These states are shown in Fig. 1. The solution (3) can be extended when there are additional vortex-antivortex pairs present [5], allowing to describe both transient dynamical states as well as finite (simple and topologically charged domain walls).

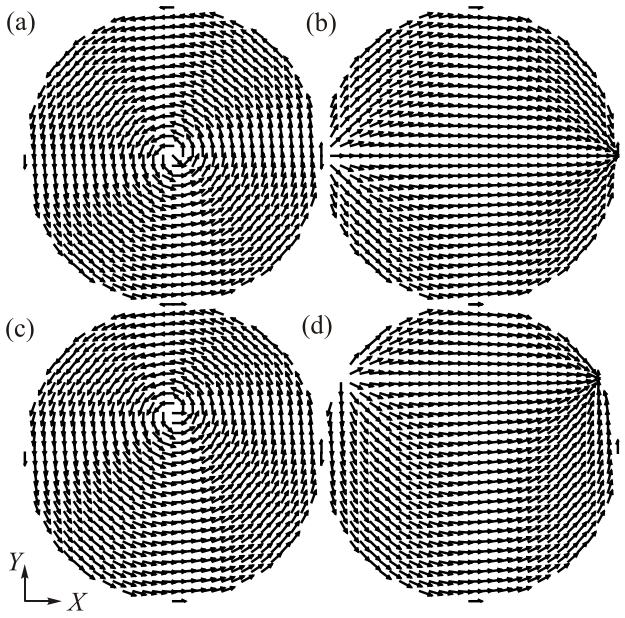

Fig. 1. Equilibrium and transient magnetization states in ferromagnetic nanodisk following from the Eq. (3): (a) centered magnetic vortex; (b) "leaf" state; (c) displaced magnetic vortex; (d) "C"-like state.

Before proceeding to the consideration of multiply-connected case, let us note a general property of the above Riemann–Hilbert boundary value problem. If it has a solution $f(z)$ in the region $z\in D$, the corresponding solution $u(t)$ in another region $t\in D'$, connected to D via the conformal mapping $t=T(z)$, can be expressed as

$$u(t) = f(z)T'(z)\big|_{z=T^{(-1)}(t)}, \quad (4)$$

where $T^{(-1)}(t)$ is the inverse of the conformal mapping $t=T(z)$, which is always defined. This expression applies both to simply- and multiply-connected cases and allows to express $u(t)$ in an arbitrarily shaped cylinder, based on its expressions $f(z)$ for some canonical domains. In the simply-connected case these canonical domains can be chosen, based on convenience only, to be the unit disk [6], the half-plane [5] or any other simply connected region for which the solution can be written explicitly. Selection of the canonical domain is trickier in the multiply-connected case, since not every pair of regions with the same connectivity can be conformally mapped into each other.

Thanks to the Koebe's theorems, it is well known that it is possible to define parametrized canonical families of multiply-connected regions, which, after parameter adjustment, can be mapped to an arbitrary region of the same connectivity. Among them is the family [10] of circular domains with cut out inner circles shown in Fig. 2.

Positions and radii of the circular holes in these domains are not arbitrary and are dictated by the shape of

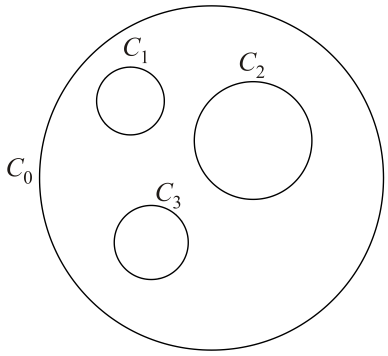

Fig. 2. An example of a quadruply-connected circular domain with an outer circular boundary C_0 and inner boundaries C_j, $j = 1, 2, 3$.

the target multiply-connected region D' to which $f(z)$ may be mapped. Because such canonical regions by themselves have physical significance (such as the simplest case of concentric ring, which is doubly-connected), let us choose them as the basis and set the goal of expressing the solutions $f(z)$ of the Riemann–Hilbert problem in these regions.

But first we need to address the question of existence of such solutions and their general properties. Formally, given a finitely connected flat domain $\mathcal{D}$ with good enough boundary (say, piecewise analytic), the problem is to find a meromorphic function $f(z)$ in the domain, satisfying the boundary condition

$$\mathrm{Re}\,(f(z)\overline{n(z)}) = 0, \quad z \in \partial\mathcal{D}, \tag{5}$$

where $n(z)$ is a normal to the boundary of the domain. The solution $f(z)$ may have zeros and polynomial singularities at the boundary. This (Riemann–Hilbert) boundary condition can be reformulated as follows:

$$\mathrm{Im}\,\frac{dz}{f(z)} = 0, \quad z \in \partial\mathcal{D}, \tag{6}$$

which means that meromorphic differential $(dz)/f(z)$ is real (i.e. the restriction of this differential to the boundary is a real differential). The latter condition is conformally invariant, which, in particular, implies (4).

To describe the set of all real differentials in $\mathcal{D}$, the useful notion is the double of the domain. The latter is a compact Riemann surface $X(\mathcal{D})$ of genus g equal to the number of the boundary components of $\mathcal{D}$ minus one. It is made of two copies of the domain glued along its boundaries, z being the conformal coordinate on one copy and $\overline{z}$ — on the other. This surface admits natural anticonformal involution $\overline{J}$ (or reflection), the interchange of copies, which is stationary exactly on the boundary components of the domain $\mathcal{D}$. The reflection acts on the differentials and the condition for the differential $d\eta$ to be real is exactly the following:

$$\overline{J}\,d\eta = \overline{d\eta}.$$

Corollary: The following topological phenomenon can be observed:

$$\#\{f(z)\ poles\} - \#\{f(z)\ zeroes\} = \#\{D\ boundaries\} - 2$$

where the poles and the zeros are counted with their multiplicities and for those at the boundary the multiplicity should be divided by two.

Proof: The solution $f(z)$ corresponds to the meromorphic differential $d\eta := (dz)/f(z)$ on the double of $\mathcal{D}$. The degree of the divisor of a differential is $2g-2$.

This implies that we can't control independently number of zeros and poles of $f(z)$.

The natural recipe to cook a real differential is symmetrization: take any meromorphic differential $d\eta$ on the surface, then its symmetrization $d\eta + \overline{J}\,\overline{d\eta}$ is meromorphic and real. This recipe is easy to use once we have a representation of the double $X(D)$ as an algebraic curve. This representation, for the case of circular multiply connected domains can be represented via a series over the elements of the corresponding Schottky group [11]. The evaluation of such series, however, can be very inconvenient if approached directly. That's why in the following we will give the representation of the solution $f(z)$ via the Schottky–Klein prime function [12,13], which not only admits an efficient numerical evaluation [14], but can also be directly used in building the conformal map $t = T(z)$ of D to D' if the latter is a multiply-connected polygonal domain [15]. It also has a number of applications in problems of optimization and computation [16,17].

Informally (for the formal definition see e.g. Ref. 14), the Schottky–Klein prime function $w(z,\zeta)$ for a specific multiply-connected circular domain D can be thought as a generalization of the difference

$$z - \zeta = w_1(z,\zeta), \tag{7}$$

which in multiply connected case becomes

$$w = w(z,\zeta). \tag{8}$$

In a simply-connected case products of such differences can be used to build the rational functions of complex variable, such as those equivalent to the set of Belavin–Polyakov solitons [2] or a similar set of states of finite nanomagnet [5], or those, entering the Schwarz–Christoffel formula for the conformal mapping of polygons. Generalization of the latter to the multiply-connected case was done by Crowdy [15], here we shall outline a generalization of the former.

In the simplest doubly-connected case of a concentric ring with an outer radius of 1 and an inner radius of $q < 1$ the Schottky–Klein prime function can be expressed as a product

$$w_r(z,\zeta) = (z-\zeta)\frac{\prod_{k=1}^{\infty}(1-q^{2k}z/\zeta)(1-q^{2k}\zeta/z)}{\left(\prod_{k=1}^{\infty}(1-q^{2k})\right)^2} \tag{9}$$

or written via the q-Pochhammer symbols $(a;q)_n$ as

$$w_r(z,\zeta) = \frac{z\zeta}{z-\zeta}\frac{(\zeta/z,q^2)_\infty (z/\zeta,q^2)_\infty}{\left((q^2,q^2)_\infty\right)^2}. \qquad (10)$$

This representation will be used in some of the following examples.

To build the solutions of the Riemann–Hilbert problem with the specified positions of vortices (or antivortices) let us define two auxiliary functions, following from those, introduced in the Sec. 5 of Ref. 15:

$$F_1(z,\zeta_1,\zeta_2) = \frac{w(z,\zeta_1)}{w(z,\zeta_2)}, \qquad (11)$$

$$F_2(z,\zeta) = \frac{w(z,\zeta)w(z,1/\bar{\zeta})}{w(z,\bar{\zeta})w(z,1/\zeta)}, \qquad (12)$$

which, provided ζ_1 and ζ_2 belong to the same inner or outer circle C_j (with $j = 0,1,2,\ldots$) of the multiply-connected circular domain and ζ is any point inside of it, have constant argument (complex phase) on all the boundaries C_j of the said domain. This means that any product of these functions will have the constant argument on the boundaries of the circular domain too, which implies that the logarithmic derivative of this product

$$g(z) = \frac{\partial}{\partial z}\log\left(\prod_m F_1(z,\zeta_{1,m},\zeta_{2,m})\prod_n F_2(z,\zeta_n)\right) \qquad (13)$$

will be an analytic function of z satisfying the condition (5) at the boundary of the multiply-connected circular domain. That is, $f(z) = g(z)$ will be a solution of the Riemann–Hilbert problem with the specified (by the parameters $\zeta_{1,m}$, $\zeta_{2,m}$, ζ_n) positions of zeros and poles. It will have some additional zeros and poles too, so that the previously mentioned topological constraint is always satisfied. Also, it is easy to show that the function $f(z) = g(1/z)$ corresponds to a "mirror" solution of the problem, where the vortices, specified by the parameters ζ, correspond to the antivortices and vice versa. This is illustrated by several examples in Figs. 3–7, some of which closely resemble well known magnetization textures, observed in ferromagnetic nanorings.

From these, the corresponding magnetization textures in the nanomagnets of the same high connectivity but other shapes can be derived according to the Eq. (4) using the conformal mapping (e.g. the mapping to the multiply-connected polygonal domains, which are also expressed in terms of Schottky–Klein prime function [15]).

Thus, we have built an approximate analytical representation of the low-energy magnetization states in planar multiply-connected nanomagnets. It is parametrized via the positions of some of vortices or antivortices in the magnet. Not all topological singularities can be freely placed. There are additional restrictions on their positions, whose number

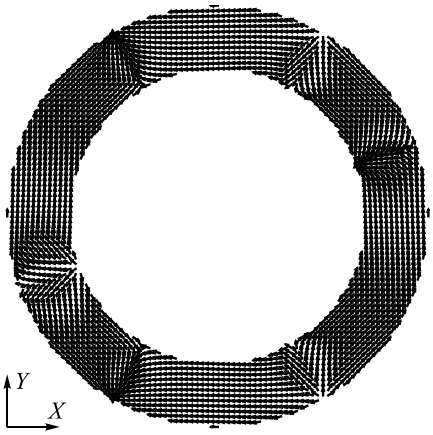

Fig. 4. A domain structure with several finite domain walls in a ring of $q = 0.7$, with $g(z)$ containing now the product of three F_1 functions: $F_1(z,e^{8\pi i/9},e^{-\pi i/9})$, $F_1(z,qe^{4\pi i/3},qe^{-2\pi i/3})$ and $F_1(z,qe^{\pi i/3},qe^{-\pi i/3})$. The rest of parameters are the same as in Fig. 3.

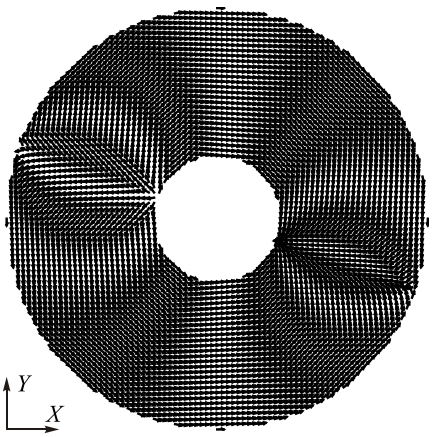

Fig. 3. Finite domain walls in a ring of $q = 0.3$, given by (1) and (2) with $e_1 = 0$, $e_2 \to \infty$, $g(z) = (\partial/\partial z)\log F_1(z,e^{-8\pi i/9},e^{\pi i/9})$ and $f(z) = g(1/z)$.

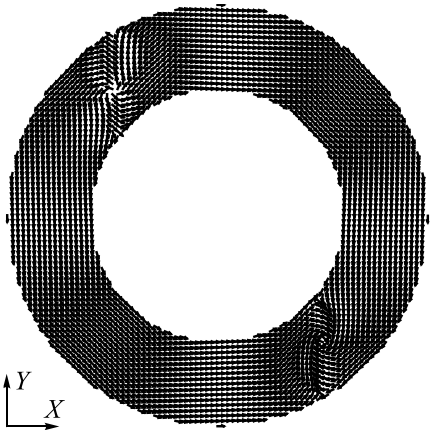

Fig. 5. Vortex domain walls in a ring of $q = 0.6$, with $g(z)$ containing the product of $F_1(z,e^{4\pi i/3},e^{\pi i/3})$ and $F_1(z,qe^{11\pi i/9},qe^{2\pi i/9})$. The rest of parameters are the same as in Fig. 3.

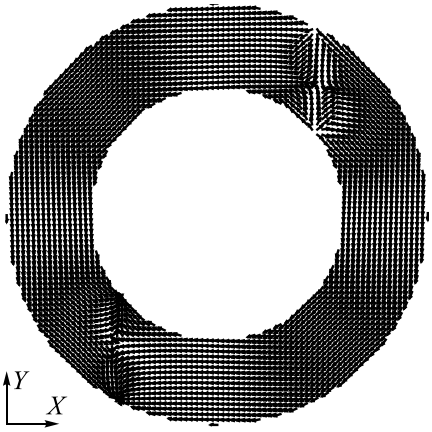

Fig. 6. Antivortex domain walls in a ring. The parameters for this plot are the same as in Fig. 5, except that now $f(z) = g(z)$.

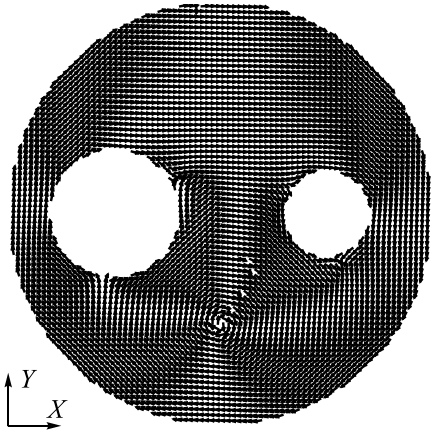

Fig. 7. A vortex in a triply connected domain, with the cut out circles of the radii 0.2 and 0.3, located at $x = 0.5$ and $x = –0.5$ respectively. The function $g(z) = (\partial / \partial z)\log F_2(z, –0.52i)$ and $f(z) = g(z)$. The Schottky–Klein prime function was evaluated numerically, using the Matlab package developed in Ref. 14.

is equal to the number of boundary components minus one. These restrictions will be discussed in our forthcoming paper. Moreover, there is a "soft" constraint on the number of vortices and antivortices in relation to the connectivity of the system, present in or near the equilibrium. It is of the same "soft" nature as the topological solitons themselves in finite systems. Really, only in the infinite 2nd magnet the topological charge is conserved and there is an infinitely high energy barrier [2], separating the states with different topological charge. In finite magnets this barrier is finite and vortices may enter/exit the particle through the boundary, changing the topological charge of the magnetization texture inside. Yet, once this barrier is holding (and the magnetization vector is pinned to the boundary of the nanomagnet) the vortices inside the planar nanoelements behave like true topological solitons.

Complete solution of the micromagnetic problems, using these parametrized magnetization textures as trial functions, will require computation and minimization of the total energy of the magnet (including the exchange, magnetostatic and other energy terms), or, solution of the equations of the magnetization dynamics using the parameters as collective variables [7]. In many cases this can be a very complex task, which is probably still easier to approach numerically (as it was done in the framework of the Magnetism@home distributed computational project [18]). Yet, even without the total energy computation, these analytical trial functions can still be useful to understand, classify and interpret the magnetization textures, obtained in the experiment and simulations. Also, they can lead to beautiful analytical results, with the generality well beyond what numerical micromagnetics may offer. Like, for example, the formula for the magnetic vortex precession frequency [19], based on the displaced vortex model (3). The presented "complex variables" approach might generate more useful models, now in multiply-connected case as well.

1. T.H.R. Skyrme, *Proc. Roy. Soc. A* **247**, 260 (1958).
2. A.A. Belavin and A.M. Polyakov, *ZETP Lett.* **22**, 245 (1975).
3. G. Woo, *J. Math. Phys.* **18**, 1264 (1977).
4. D.J. Gross, *Nuclear Phys. B* **132**, 439 (1978).
5. K.L. Metlov, *Phys. Rev. Lett.* **105**, 107201 (2010).
6. K.L. Metlov, *Two-dimensional Topological Solitons in Soft Ferromagnetic Cylinders* (2001), *arXiv:cond-mat/0102311*.
7. K.L. Metlov, *Phys. Rev. B* **88**, 014427 (2013).
8. K.L. Metlov, *J. Appl. Phys.* **114**, 223908 (2013).
9. K.L. Metlov and Y.P. Lee, *Appl. Phys. Lett.* **92**, 112506 (2008).
10. P. Koebe, *Acta Mathematica* **41**, 305 (1914).
11. F. Schottky, *J. Reine Angew. Math.* **83**, 300 (1877).
12. F. Schottky, *J. Reine Angew. Math.* **101**, 227 (1887).
13. F. Klein, *Math. Ann.* **36**, 1 (1890).
14. D. Crowdy and J. Marshall, *Computational Methods and Function Theory* **7**, 293 (2007).
15. D. Crowdy, *Proc. R. Soc. A* **461**, 2653 (2005).
16. A.B. Bogatyrev, *Computational Methods and Function Theory* **7**, 309 (2007).
17. A.B. Bogatyrev, *Computational Methods and Function Theory* **9**, 47 (2009).
18. K.L. Metlov, *J. Appl. Phys.* **113**, 223905 (2013).
19. K.Y. Guslienko, X.F. Han, D.J. Keavney, R. Divan, and S.D. Bader, *Phys. Rev. Lett.* **96**, 067205 (2006).